J|A|C|S
ARTICLES
Published on Web 12/01/2006

Potential of Mean Force for Tetramethylammonium Binding to Cagelike Oligosilicates in Aqueous Solution

S. Caratzoulas,*,† D. G. Vlachos,† and M. Tsapatsis‡

Contribution from the Department of Chemical Engineering, University of Delaware, Newark, Delaware 19716, and Department of Chemical Engineering & Materials Science, University of Minnesota, 421 Washington Avenue SE, Minneapolis, Minnesota 55455

Received June 28, 2006; E-mail: cstavros@udel.edu

Abstract: We have carried out free energy calculations to compute the potential of mean force for the cagelike silicate polyion−TMA^+ cation ion pair interaction in aqueous solution. We also have studied solvent reorganization-related entropic effects. We conclude that the organocations, as opposed to, for example, alkali-metal ions, play a pivotal role in reorganizing the solvent around the cagelike silicates in a manner conducive to the formation of heteronetwork clathrates that are stable both thermodynamically and kinetically. In the case of stable cagelike polysilicate anions, this solvent reorganization correlates with entropic losses. We also infer that transient cagelike polysilicate species, that may indeed form but participate in floppy clathrates, eventually have to give way to cagelike polysilicates that lead to more rigid structures.

I. Introduction

Zeolite crystallization assisted by organic cations (typically tetraalkylammonium cations (TAA)) involves complex solution chemistry. A host of modern analytical and computational techniques have been applied in studies that aim to obtain better understanding of the molecular processes that take place.[1−7] The role of the organic cations remains enigmatic, and controversy surrounds aspects of their function. We have taken interest in the problem and tried to elucidate some of the outstanding issues using molecular simulation.

The template model—the organocations organize the framework formation around them, determine the pore architecture, and minimize the energy of the inorganic framework by neutralizing excess charge[5,6,8,9]—is deeply rooted in the structural fragment condensation theory for zeolite nucleation and growth in solution. The theory accepts the existence of secondary building units (SBU) which readily self-assemble to yield the final crystal structures. Over the years, the template model has received some endorsements, but now mostly criticism. The problem is that only a handful of frameworks fit the model,[10] and computational approaches that have been based on it have not met with much success.[5]

Appealing as the SBU theory may sound, unfortunately many of its underpinning assumptions have been refuted. The problem is that ^{29}Si-NMR spectra of aqueous silicate solutions are, in principle, consistent with the structures of an almost infinite number of silicate anions.[11] This has led to many unfounded structural assignments, especially by proponents of the structural fragment condensation theory. The open and flexible, five-, six-, and eight-member ring systems of the SBUs are unknown in aqueous solutions. On the contrary, silicate anions tend to be as highly condensed as possible.[11−17] Through NMR methods, the structures of the principal silicate anions found in aqueous alkaline solution have been determined, as has the cation's influence on silicate speciation. In fact, the silicate solutions are composed of many small, highly condensed molecules in dynamic equilibrium, with relative concentrations governed by the laws of polymer chemistry.[11]

One of the most dramatic examples of silicate speciation is the dominance of the cubic octamer, Q_8^3, in solutions prepared with TAA cations having alkyl group chain lengths of three or less. The octamer forms at an anomalously slow rate. As the Q_8^3 concentration increases, that of the prismatic hexamer, Q_6^3,

† University of Delaware.
‡ University of Minnesota.

(1) Kirschhock, C. E. A.; Ravishankar, R.; Jacobs, P. A.; Martens, J. A. *J. Phys. Chem. B* **1999**, *103*, 11021−11027.
(2) de Moor, P. P. E. A.; Beelen, T. P. M.; Komanschek, B. U.; Beck, L. W.; Wagner, P.; Davis, M. E.; van Santen, R. A. *Chem.—Eur. J.* **1999**, *5*, 2083−2088.
(3) Mintova, S.; Olson, N.; Bein, T. *Angew. Chem., Int. Ed.* **1999**, *38*, 3201.
(4) Catlow, C.; Coombes, D.; Lewis, D.; Pereira, J. *Chem. Mater.* **1998**, *10*, 3249.
(5) Lewis, D.; Willock, D.; Catlow, C.; Thomas, J. M.; Hutchings, G. *Nature* **1996**, *382*, 604.
(6) Wu, M.; Deem, M. *J. Chem. Phys.* **2004**, *116*, 2125.
(7) Jorge, M.; Auerbach, S.; Monson, P. *J. Am. Chem. Soc.* **2005**, *127*, 14388−14400.
(8) de vos Burchart, E.; Jansen, J.; van der Graaf, B.; van Bekkum, H. *Zeolites* **1993**, *13*, 216.
(9) den Ouden, C.; Datema, K.; Visser, F.; Mackay, M.; Post, M. *Zeolites* **1991**, *11*, 418−424.
(10) Lai, Z.; Bonilla, G.; Nery, G.; Diaz-Carretero, I.; Sujaoti, K.; Amat, M. A.; Kokkoli, E.; Terasaki, O.; Thompson, R. W.; Tsapatsis, M.; Vlachos, D. G. *Science* **2003**, *300*, 456−460.
(11) Knight, C. T. G.; Kinrade, S. D. *J. Phys. Chem. B* **2002**, *106*, 3329.
(12) Harris, R. K.; Knight, C. T. G. *J. Chem. Soc., Faraday Trans. 2* **1983**, *79*, 1525.
(13) Harris, R. K.; Knight, C. T. G. *J. Chem. Soc., Faraday Trans. 2* **1983**, *79*, 1539.
(14) Knight, C. T. G. *J. Chem. Soc., Dalton Trans.* **1988**, 1457.
(15) Kinrade, S. D.; Swaddle, T. *Inorg. Chem.* **1988**, *27*, 4259.
(16) Kinrade, S. D.; Knight, C. T. G.; Pole, D. L.; Syvitski, R. *Inorg. Chem.* **1998**, *37*, 4272−4277.
(17) Kinrade, S. D.; Knight, C. T. G.; Pole, D. L.; Syvitski, R. *Inorg. Chem.* **1998**, *37*, 4278−4283.

10.1021/ja064597f CCC: $33.50

(as well as of several other cagelike anions) drops, passing through a maximum in the early stages of this process.[11,16,17] In the case of concentrated tetramethylammonium (TMA) or tetrapropylammonium (TPA) silicate solutions, although the prismatic hexamer forms prior to the cubic octamer, the latter is known to be the predominant equilibrium species. In fact, stabilization of the hexamer requires a good deal of coercion—TEA (tetraethylammonium) and TMA in equal amounts and a cosolvent (usually methanol).[12,13,16−19] (For a picture of the structure of Q_8^3 or Q_6^3, see Figures 2 and 7, respectively.)

Indubitably, the organocations play a pivotal role in the preferential stabilization of some of these species. In terms of understanding the molecular level mechanism of zeolite formation, it is important to elucidate that role. The physical or chemical mechanisms that control the nature of silicate hydrates of quaternary ammonium cations obviously also influence the nature of subcolloidal zeolite nanoparticle precursors.[20−24] Furthermore, it is not unreasonable to expect that these mechanisms should also control zeolite evolution over longer time scales. In that respect, very useful supporting information may come from the study of these species, which structurally may be considered as host−guest systems (heteronetwork clathrates).[25−27]

The crystallographic work of Wiebcke et al.[25−27] and the NMR work of Kinrade et al.[16,17] on the structure and growth of the cagelike species $Si_8O_{20}^{8-}$ (cubic octamer) and $Si_6O_{15}^{6-}$ (prismatic hexamer) have recently motivated us to study these species using molecular dynamics simulations.[28,29]

The picture that has emerged from our simulations, so far, suggests a strong correlation between the stability of Q_8^3 or Q_6^3 and their ability to support a full, stable layer of TMA^+ cations. That such a relation should exist had been hypothesized, by Kinrade and co-workers,[16,17] but proven difficult to check experimentally. The analytical techniques (SANS or SAXS) are not sensitive enough to "see" these species (Q_8^3 or Q_6^3) in solution, let alone resolve one's structure or probe its surface. The claim has been that, because of the TAA's hydrophobic character, a layer of TAA cations shields the cagelike polysilicate anions from the bulk solution, impeding hydrolysis. Molecular simulation has proved very useful in this respect. Indeed, our simulations show that one of the consequences of the formation of a TMA^+ layer is that water molecules in the vicinity of the silicate bridge oxygens will get displaced.[28,29]

We have found that only Q_8^3 is surrounded by a full layer of TMA^+ cations. On the average, the layer consists of six TMA^+ cations—one cation opposite each *face* of the cubic structure.[28] Under conditions favoring Q_8^3 formation, our simulations showed only a partially formed layer around Q_6^3. On the average, the layer around the hexamer consists of fewer than three TMA^+ cations, preferentially coordinated opposite the four-ring faces of the prismatic structure, leaving the three-ring faces exposed to the bulk solution.[29]

In regard to the solvation waters of the polysilicate anions, we have found it important to stratify them into those (dubbed "polar") that participate in strong hydrogen bonds with the anionic sites (silanol oxygens) of the polysilicates and those (dubbed "nonpolar") that belong to the solvation spheres of the organic cations in the layer. Remarkably, the polar waters appear rather impervious to the presence of the layer. Analysis of their hydrogen-bond statistics revealed that *the number of hydrogen bonds they form is the same regardless of whether the silicate polyion is "bare" (no TMA^+ layer) or "dressed."* Specifically, if we count both water−water and water−silicate H-bonds, the average number of H-bonds per polar solvent molecule turns out almost equal to that in the bulk solution. There are fewer water−water hydrogen bonds than in the bulk because the polar water's bonds are orientated toward the negatively charged silanol oxygens.

These H-bond statistics are common to both the octamer and the hexamer but with one very important caveat. In the case of the hexamer, to analyze the H-bond statistics associated with the dressed polyion, the layer was *mathematically constrained* at its surface and not let dissolve in the course of the simulation.[29]

Our studies have also shown that a TMA^+ layer has a profound effect on the kinetics of the water−oligosilicate hydrogen bonds: their lifetimes increase by at least a factor of 2.[29] It transpires that a TMA^+ layer not only serves as the putative "protective shield," but also *contributes to the kinetic stability of the local, water−organic environment hosting the polyion.* So, the hydrates of the octamer and the hexamer may have very similar clathrate-like structures with respect to the structure of the local solvent, but they also differ in one very significant respect: this clathrate structure is kinetically more stable in the case of the octamer because the octamer can support a TMA^+ layer at its surface whereas the hexamer cannot.

Thus, we have correlated the stability of a cagelike polysilicate with its ability to support a full layer of organic cations. We have also related the presence of this layer with the enhanced kinetic stability of the clathrate heteronetwork hosting the silicate polyion. Intuitively, one expects that this kinetic stability should be the result of reduced solvent mobility, with concomitant entropic costs. In this article, we shall have the opportunity to investigate solvent mobility as it relates to TMA binding. This is an important issue, not only because it is relevant to the problem of the stabilization of organosilicate complexes in aqueous environments but also because it is relevant to the growth problem and how these organosilicate particles interact with each other. In our previous work, we alluded to the possibility that a TMA layer may give a silicate polyion partly hydrophobic character. If this turns out to be the case here, one should expect clearer manifestations of hydrophobicity in systems with TAAs with longer alkyl groups.

In our studies, up to this point, the stability of the layer has been inferred from ns-long molecular dynamics trajectories with

(18) Knight, C. T. G.; Kirkpatrick, R. J.; Oldfield, E. J. *J. Am. Chem. Soc.* **1986**, *108*, 30.
(19) Knight, C. T. G.; Kirkpatrick, R. J.; Oldfield, E. J. *J. Am. Chem. Soc.* **1987**, *109*, 1632.
(20) Fedeyko, J. M.; Rimer, J. D.; Lobo, R. F.; Vlachos, D. G. *J. Phys. Chem. B* **2004**, *108*, 12271−12275.
(21) Fedeyko, J.; Sawant, K.; Kragten, D.; Vlachos, D.; Lobo, R. *Stud. Surf. Sci. Catal.* **2004**, *154*, 1267−1273.
(22) Fedeyko, J.; Vlachos, D.; Lobo, R. *Langmuir* **2005**, *21*, 5197−5206.
(23) Rimer, J.; Vlachos, D.; Lobo, R. F. *J. Phys. Chem. B* **2005**, *109*, 12762−12771.
(24) Rimer, J.; Lobo, R.; Vlachos, D. *Langmuir* **2005**, *21*, 8960−8971.
(25) Wiebcke, M.; Hoebbel, D. *J. Chem. Soc., Dalton Trans.* **1992**, 2451−2455.
(26) Wiebcke, M.; Grube, M.; Koller, H.; Engelhardt, G.; Felsche, J. *Microporous Mater.* **1993**, *2*, 55−63.
(27) Wiebcke, M.; Felsche, J. *Microporous Mesoporous Mater.* **2001**, *43*, 289−297.
(28) Caratzoulas, S.; Vlachos, D.; Tsapatsis, M. *J. Phys. Chem. B* **2005**, *109*, 10429.
(29) Caratzoulas, S.; Vlachos, D.; Tsapatsis, M. *J. Am. Chem. Soc.* **2006**, *128*, 596−606.

various initial conditions (i.e., preparations of $Q_n^3 \cdot m$ TMA (n = 6, 8) complexes in solution) and the resulting equilibrium distributions of the cations around the silicate polyions.[28,29] For the hexamer, all initial conditions resulted in (partial) dissolution of the layer, and thereby we spoke of an unstable layer. On the other hand, in the case of the octamer, all initial conditions led to trajectories that most of the time were trapped in a basin of the multidimensional potential that corresponds to the state in which the six organocations are bound to the surface.

In this article, we investigate the energetics of the layer stability in more direct fashion. To that end, we associate stability with the binding strength of a layer counterion. This perspective has been motivated by the dynamics of the systems. According to them, the dissolution of the layer begins with the first TMA^+ that leaves the pack. As a result, water creeps up to the surface. As soon as surface "wetting" sets in, some, not all, of the remaining cations leave the surface and transfer to the bulk.[29]

Here, we study this binding strength by carrying out free-energy calculations to compute the mean force between the silicate polyion−TMA^+ cation ion pair as a function of their separation R. This direct approach will also permit us to study entropic effects as they relate to solvent reorganization.

Finally, we shall investigate the silicate−organic cation ion pair interaction in the presence of alkali-metal cations. Our results from this system make direct contact with experimental observations and put the "scaffolding" theory on much firmer footing.

II. Simulation Details

The change in free energy due to a reversible perturbation from an equilibrium state where two molecules are a distance R_0 apart to an equilibrium state where their separation is R_1 is given by

$$\beta\Delta F(R_1; R_0) = -\ln\langle\exp[-\beta(E(R_1) - E(R_0))]\rangle_{R_0} \qquad (1)$$

where $\beta^{-1} = k_B T$, k_B is Boltzmann's constant, T is temperature, and $\langle\cdots\rangle_{R_0}$ denotes ensemble average over the equilibrium states corresponding to R_0. The quantity $\Delta F(R_1;R_0)$ is the potential of mean force (pmf) between two molecules separated by R_1. For the actual computation, we have employed the finite difference thermodynamic integration (FDTI) method,[30]

$$\Delta F(R_1;R_0) = \int_{R_0}^{R_1} \frac{\partial F}{\partial R}\,\mathrm{d}R = \sum_i w_i \left(\frac{\partial F}{\partial R}\right)_{R=R_i} \qquad (2)$$

where R_i are Gaussian quadrature integration points and the derivative $(\partial F/\partial R)_{R=Ri}$ is computed via the centered difference

$$(\Delta F(R_i + \delta R;R_i) - \Delta F(R_i - \delta R;R_i))/(2\delta R)$$

with the $\Delta F(R_i \pm \delta R;R_i)$ computed via eq 1.

Within the FDTI framework, the entropic contributions to the free-energy change associated with the perturbation $R_0 \rightarrow R_1$ of eq 2 have been calculated by[31]

$$-T\Delta S(R_1;R_0) = \beta \int_{R_0}^{R_1} \left(\left\langle E\frac{\partial E}{\partial R}\right\rangle_R - \langle E\rangle_R \left\langle \frac{\partial E}{\partial R}\right\rangle_R\right)\mathrm{d}R \qquad (3)$$

(30) Mezei, M. *J. Chem. Phys.* **1987**, *86*, 7084−7088.
(31) Smith, D. E.; Haymet, A. D. J. *J. Chem. Phys.* **1993**, *98*, 6445−6454.

Table 1. Intermolecular Potential Parameters

atom	ϵ (kcal/mol)	σ (Å)	q
	Water[a]		
O	0.1521	3.1501	−0.834
H	0.0	0.0	0.417
	Tetramethylammonium (TMA)[b]		
N	0.17	3.25	0.289
C	0.12	3.29	−0.302
H	0.02	1.78	0.160
	Silica Hexamer ($Si_6O_{15}^{6-}$)[b]		
Si	0.04	4.053	1.77
O_b[c]	0.105	3.35	−1.04
O_t[c]	0.105	3.35	−1.22
	Silica Octamer($Si_8O_{20}^{8-}$)[b]		
Si	0.04	4.053	1.55
O_b[c]	0.105	3.35	−0.875
O_t[c]	0.105	3.35	−1.22
	Sodium Ions in Water		
Na[d]	1.6071	1.8974	1

[a] TIP3P, ref 35. [b] Partial charges, this work; Lennard-Jones parameters from CFF. [c] O_b siloxane, bridge oxygen; O_t silanol, terminal oxygen. [d] Reference 36.

To ensure sufficient overlap between reference equilibrium states, in all the calculations the R-range was divided into windows of length ΔR = 0.4 Å with four reference states per window, corresponding to four Gaussian quadrature integration points per window. For R ranging from 5.5 to 11.5 Å, 60 reference states were considered in all. For the finite differences we have used δR = 0.05 Å.

Equilibrium configurations in each reference state were harvested using molecular dynamics in the *NVT* ensemble at T = 300 K. Each reference state was equilibrated for 50ps with Nosé-Hoover thermostat. Configurations were subsequently stored every 2 fs during a 20 ps observation period, with the thermostat turned off.

Equilibration and sampling at each reference state were checked via the distribution of the work values associated with the R "switches" of length δR. At or near equilibrium, these work values should follow a normal distribution with dispersion related to the dissipated work.[32]

Statistical errors are reported for the free-energy estimates within each window of length ΔR = 0.4 Å; they are estimated using block averaging.[33,34]

In all the simulations reported on here, we used a cubic simulation box of lattice constant 27.3 Å, with periodic boundary conditions. The solvent consisted of 670 water molecules.

The force field for intermolecular interactions was based on pairwise additive potentials between atomic sites:

$$u_{\alpha\beta}(r) = \frac{q_\alpha q_\beta}{r} + 4\epsilon_{\alpha\beta}\left[\left(\frac{\sigma_{\alpha\beta}}{r}\right)^6 - \left(\frac{\sigma_{\alpha\beta}}{r}\right)^{12}\right] \qquad (4)$$

where α and β denote a pair of interacting sites on different molecules, r is the separation between two interacting sites, q_α is the point charge at site α, and $\epsilon_{\alpha\beta}$ and $\sigma_{\alpha\beta}$ are, respectively, the energy and distance parameters in the Lennard-Jones potential. The electrostatic interactions were treated using Ewald summation. The force field parameters used in this work are given in Table 1.

Each of the potential of mean force calculations required an average of 1800 CPU hours.

III. Results

A. Octamer. For the bare polysilicate anion−TMA^+ cation ion pair we expect a net attractive force determined primarily

(32) Gore, J.; Bustamante, C. *Proc. Natl. Acad. Sci. U.S.A.* **2003**, *100*, 12564−12569.
(33) Flyvbjerg, H.; Petersen, H. *J. Chem. Phys.* **1989**, *91*, 461−466.
(34) Ytreberg, F.; Zuckerman, D. *J. Comp. Chem.* **2004**, *25*, 1749−1759.
(35) Jorgensen, W. L. *J. Chem. Phys.* **1982**, *77*, 4156.
(36) Chandrasekhar, J.; Spellmeyer, D.; Jorgensen, W. L. *J. Am. Chem. Soc.* **1984**, *106*, 903−910.

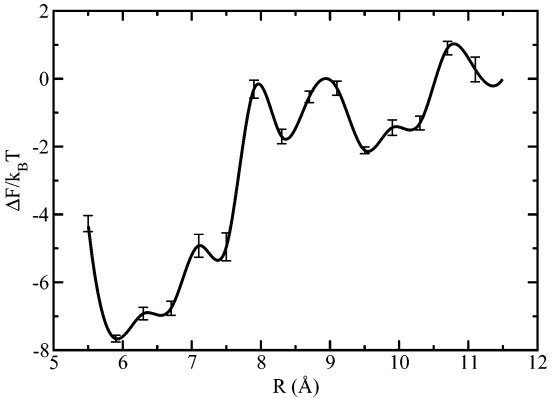

Figure 1. Potential of mean force for the TMA^+ cation−bare cubic octamer ion pair interaction in aqueous solution, as a function of the pair's separation R. The error bars correspond to the free energy changes calculated by Gaussian quadrature within each window of length $\Delta R = 0.4$ Å.

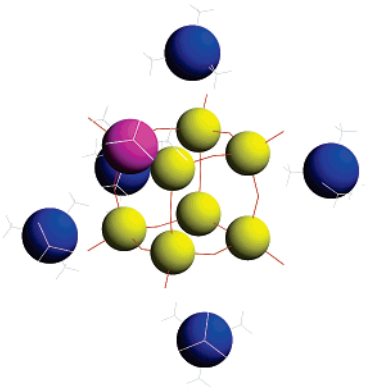

Figure 2. Ball-and-stick image of the cubic octamer with six TMA cations: yellow balls, Si atoms; blue balls, N atoms of the restrained TMA cations; magenta ball, N atom of the tagged *TMA* cation that is reversibly pulled off the surface; red sticks, oxygen atoms; and gray sticks, TMA methyl groups. The image is taken from a molecular dynamics trajectory at the value $R = 9.0$ Å of the reaction coordinate. Here, the tagged *TMA*, initially coordinated opposite a face of the cubic octamer, is located almost along the C_3 symmetry axis, i.e., the cube's diagonal.

by electrostatics. Solvent should also reorganize (move out of the way and reorientate) as TMA gets closer to the surface. This is water in the solvation sphere of the organocation or silicate hydration water coordinated opposite the face TMA binds to; TMA loses about 50% of its solvation water. In the case of the bare octamer, the calculated pmf, $\Delta F(R)$, for this interaction is shown in Figure 1. The state with TMA bound to the surface, at $R = 6.0$ Å, is stabilized by $\sim 8 k_B T$ (4.7 kcal/mol) relative to the state at $R = 11.5$ Å.

How does this force change when the TMA is one of the six making up the octamer's layer of counterions? For this calculation, six TMA cations were let equilibrate at the surface of the octamer (one per face). The entire complex was then immersed in water and underwent energy minimization and re-equilibration. Five of the six TMAs were subsequently restrained to remain at the surface while the sixth one (tagged *TMA*) was reversibly being pulled off (see Figure 2.) For electroneutrality, two Na^+ were included in the simulation box.

The five TMA cations were restrained at the surface to ensure that we calculate the reversible work to pull the *first* TMA cation off the surface. As we mentioned in the Introduction, this perspective has been motivated by our previous work, according to which the dissolution of the layer initiates with the first TMA^+ that leaves the surface.[29] Furthermore, the statistical fact that, on the average, six TMAs are bound to the surface does not preclude the possibility of a cation's brief sojourn off the surface and into the bulk, because of thermal fluctuations. Thus, because, in general, the reversible work to remove the first TMA from the surface will not be equal to the work to remove the second TMA, etc., the information we wished to extract from these calculations dictated that we restrain the remaining five TMAs at the surface. In practice, we fixed the separation between the center of mass of the octamer and the center of mass of each of the five TMAs.

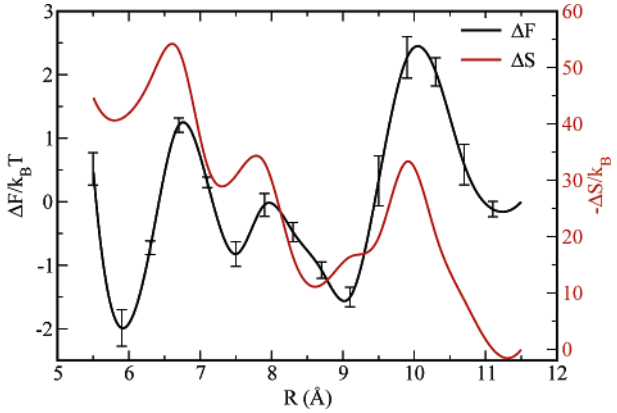

Figure 3. Potential of mean force, $\Delta F(R)$, for the TMA^+ cation−"dressed" cubic octamer ion pair as a function of the pair's separation R, in aqueous solution containing six TMA^+ and two Na^+ cations (black line). The red line depicts the entropic term, $-T\Delta S$ (R), and is drawn on the right-hand scale. (Error bars same as in Figure 1.)

The potential of mean force as a function of the *TMA*−octamer separation, R, is given in Figure 3. The stationary point at $R \approx 6.0$ Å is the global minimum of $\Delta F(R)$ and naturally corresponds to a thermodynamically stable state. The barrier to remove it from the surface, and of course from the layer, is about 3.5 $k_B T$, higher than the average thermal energy but significantly lower than the barrier in the pmf between TMA and the bare polyion (cf. Figure 1). In Figure 3, there are also two local minima, at $R \approx 7.5$ and 9.0 Å, separated by a low barrier (~ 0.5 $k_B T$ moving outward). The structure of ΔF (R) is partly due to solvent reorganization and partly due to the TMA being free to rotate and reorientate relative to the octamer, at fixed R. At small R (*TMA* at the surface or close to it), the organocation is coordinated opposite a face of the cubic polysilicate and, as R grows, it moves, on the average, along the normal to that face (C_4 symmetry axis). Near the barrier at $R \approx 6.7$ Å its path starts to diverge from the direction of the normal. The local minimum at $R \approx 7.5$ Å corresponds to an ensemble of configurations with the *TMA* in the vicinity of one of the (C_2) diagonals connecting opposite edges of the cubic silicate, at about 45° from its original direction. At the $R \approx 9.0$ Å local minimum, the cation is, on the average, coordinated along the C_3 symmetry axis, approximately at a 55° angle from its original direction.

In Figure 3, the red line is the graph of the entropic contribution $-T\Delta S(R)$, computed with the method described in section II. The entropic term variations with R closely follow those of $\Delta F(R)$. Overall, TMA binding entails an entropic cost of $\Delta S_{bind}/k_B \approx -40$ (about -79.5 cal/(mol K)). This is part ligand translational and rotational freedom losses, ascribed to binding, and part solvent reorganization.

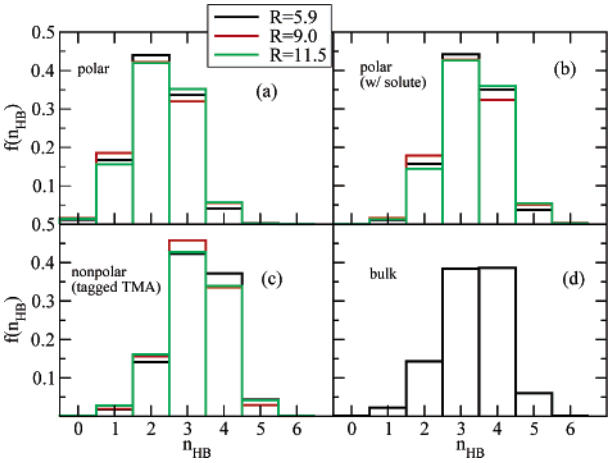

Figure 4. Fraction, $f(n_{HB})$, of water molecules participating in n_{HB} hydrogen bonds at three values of the octamer−TMA separation R (in Å). The water molecules have been grouped according to their time-averaged proximity to the "polar" (O and O^-) and "nonpolar" (CH_3) functional groups of the solutes: (a) water molecules that, on the average, spend most of their time in the hydration sphere of the octamer; (b) same as in panel a but in addition to the water−water H-bonds we count the water−octamer H-bonds; (c) water molecules in the hydration sphere of the tagged *TMA* being moved relative to the octamer; (d) water molecules in the bulk.

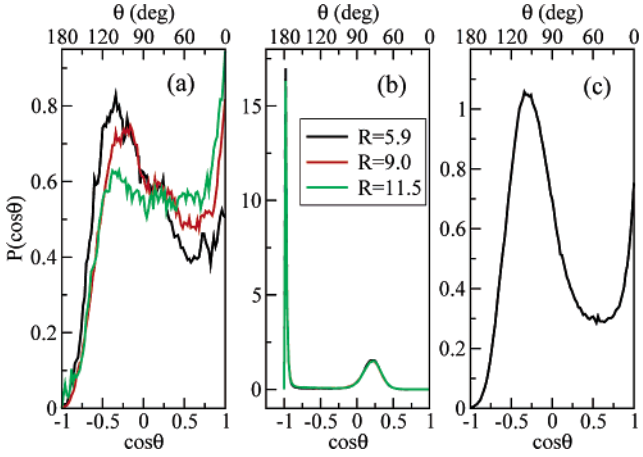

Figure 5. Distribution of orientations of water molecules, at various octamer−*TMA* separations R (in Å): (a) water near the methyl groups of the moving TMA ("nonpolar" water); (b) water in the hydration sphere of the octamer and immediate vicinity of the silicate oxygens ("polar" water); and (c) nonpolar water in the solvation shells of the five TMAs that remain bound to the surface of the octamer.

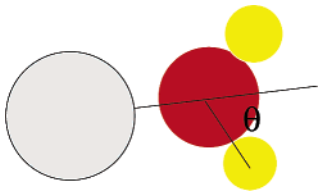

Figure 6. Schematic representation of water molecule orientation near a methyl group. (Red ball, water oxygen; yellow ball, water hydrogen; gray ball, methyl group carbon atom, silicate oxygen atom, or sodium atom, depending on context.)

It is possible to obtain estimates, albeit rough, for the ligand related entropy changes.[37−40] Because in our simulations TMA has been assumed rigid, for the translational binding entropy we use the gas-phase equation

$$\frac{S_t}{k_B N} = \frac{3}{2} + \ln\left(\frac{N\Lambda^3}{V}\right) \tag{5}$$

while for the rotational entropy we similarly employ the gas-phase equation

$$\frac{S_r}{k_B N} = \ln\left[\frac{\pi^{1/2} e^{3/2}}{\sigma}\left(\frac{8\pi^2 k_B T}{h^2}\right)^{3/2}\sqrt{I_A I_B I_C}\right] \tag{6}$$

In the above, V is volume, $\Lambda = h/(2\pi m k_B T)^{1/2}$ is the thermal de Broglie wavelength, I_i is the moment of inertia with respect to the ith principal axis, and σ is a symmetry factor. For TMA, $I_A \approx I_B \approx I_C \approx 108.3$g/(mol Å^2) and $\sigma = 12$. Hence the losses are estimated at

$$S_t/k_B N \approx -17.4 \quad \text{and} \quad S_r/k_B N \approx -10.4.$$

Both numbers are overestimates—S_t in particular, since in condensed phases the "free volume" for translational motion is smaller than in gases.[39] Furthermore, binding does not necessarily entail either total loss of the translational degrees of freedom or total loss of rotational motion. In the bound state, the ligand may still undergo translational motion, but over a smaller phase space volume, undergo purely vibrational motion, or finally retain some rotational freedom, for example, librations.

With regard to the solvent related entropy change, we have already noted that the solvent structure and H-bond network around the silicate polyion are quite robust.[29] The histograms in Figure 4 show the fractions, $f(n_{HB})$, of water molecules that participate in n_{HB} hydrogen bonds and how they vary with R. The water molecules have been classified into "polar," "nonpolar" and "bulk" according to their time-averaged proximity to the various functional groups of the solutes (Si−O−Si and Si−O^- for polar, CH_3 for nonpolar).[29,41] (The fractions $f(n_{HB})$ are calculated for solvent molecules within each group but include hydrogen bonds among water molecules in different groups.) The number of water molecules that, on the average, spend their time in the octamer's hydration sphere varies little with R and so does the average total number of H-bonds in which they participate. On the other hand, as R varies from 11.5 to 5.9 Å, the number of water molecules that spend most of their time in *TMA*'s hydration sphere changes substantially, from 31 to 15, because water has to be displaced for binding to occur. However, the histogram in panel c of Figure 4 shows that $f_{nonpolar}(n_{HB})$ changes very little with R, in a remarkable demonstration of the solvent's resilience at maintaining its H-bond network. We shall presently show that this entails a drop in the entropy of the system.

In Figure 5, panel a, we show the distribution $P(\cos\theta)$ of the angle θ between *any* of the water O−H bonds and the axis defined by the *TMA*'s methyl carbon atom closest to the water molecule and that water's oxygen atom (cf. Figure 6). In general, the maximum number of favorable water−water interactions can occur if none of the hydrogen atoms or lone-pair orbitals of the water molecule is directed toward the nonpolar group; the ideal orientation corresponds to $\theta = 0$.[42] This molecular orientation is typical of crystalline clathrate hydrate compounds,

(37) Page, I. *Angew. Chem., Int. Ed. Engl.* **1977**, *16*, 449−459.
(38) Finkelstein, A.; Janin, J. *Protein Eng.* **1989**, *3*, 1−3.
(39) Amzel, L. *Proteins* **1997**, *28*, 144−149.
(40) McQuarrie, D. A. *Statistical Mechanics;* Harper & Row: New York, 1976.
(41) Rossky, P. J.; Karplus, M. *J. Am. Chem. Soc.* **1979**, *101*, 1913−1937.

and $\theta = 0$ characterizes all of the water molecules in an ideal structure I geometry (found in crystals containing the smaller nonpolar guest molecules, e.g., CH_4). For other clathrate crystals, however, a number of water molecules can be oriented so that $\theta \neq 0$, but in each such case the orientation is such that θ is far from 180°.[42,43] All three curves of Figure 5, panel a, show the clear orientational bias of charges away from the nonpolar group. It is also evident that there is significant dispersion in the orientations found in solution; contributions from nonoptimal orientations (e.g., that involving the two O−H bonds bridging the methyl group) are clearly important. Specifically, at $R = 11.5$ Å (green curve), the distribution of orientations is very close to uniform for $-0.5 < \cos\theta < 0.8$, with some bias in the region $0.8 < \cos\theta \leq 1$. At this R, the water molecules have significant orientational freedom, over a wide range of angles θ, but also a substantial number of them are oriented with the O−H bond pointing away from the methyl group. At the intermediate value $R = 9.0$ Å (red curve), $P(\cos\theta)$ becomes more biased, with two peaks: one around $\cos\theta = 1$, and a broad, second peak at $\cos\theta \approx -0.25$. Roughly speaking, two orientations are predominant here: one is the optimal, with the O−H bond pointing away from the methyl group, and the other is with the O−H bonds bridging the *TMA*'s methyl group. This change in $P(\cos\theta)$ is accompanied by a rather small increase in the fraction of "nonpolar" water molecules participating in three hydrogen bonds (cf. Figure 4, panel c). The distribution of orientations changes further when the *TMA* binds to the surface of the octamer. The $R = 5.9$ Å (black) curve in Figure 5, panel a, shows a clear bias around the rather broad peak at $\cos\theta = -0.25$ and a vestige of the peak at $\cos\theta = 1$. Here, most of *TMA*'s solvation waters are oriented with their bonds bridging the methyl group, and much fewer than before have their O−H bonds pointing away from it.

Thus, the *TMA* solvation waters keep their H-bond network mostly unaffected at the cation's approaching of the octamer, but they reorganize into configurations with less orientational freedom. Hence, the observed entropy drop.

Two important notes are considered: First, the analogous distribution of orientations of polar water molecules (i.e., water molecules in the hydration spheres of the silicate oxygens) is virtually independent of R. In Figure 5, panel b, we show the polar $P(\cos\theta)$ at the same three R values considered above. All three curves overlap with each other. (In this case, the angle θ is defined with respect to the axis defined by the octamer oxygen closest to the water molecule and that water's oxygen atom.) The polar distribution basically consists of the high, sharp peak at $\cos\theta \approx -1$; the water O−H bonds are directed toward the anionic oxygens and form strong hydrogen bonds. This distribution is typical of all silicate systems investigated in this paper. Second, the hydration molecules of the five, surface-bound TMAs do not reorganize as the tagged *TMA* approaches the octamer. A typical distribution of the orientations of these waters is given in Figure 5, panel c.

B. Hexamer. Turning our attention to the prismatic hexamer, we have performed the same calculations to obtain the potential of mean force for the TMA^+−Q_6^3 ion pair interaction. For this calculation, five TMA cations were let equilibrate at the surface of Q_6^3 (one per face). The entire complex was then immersed in water and underwent energy minimization and re-equilibration. Four of the five TMAs were subsequently restrained to remain at the surface while the fifth one (tagged *TMA*) was reversibly being pulled off (cf. Figure 7). The restraints were handled in the same fashion as in the case of the octamer. For electroneutrality, one Na^+ was included in the simulation box. Structural studies from equilibrium molecular dynamics simulations have shown that TMA^+ prefers to be opposite four-ring rather than three-ring faces.[29] So, we have selected to calculate the reversible work to remove the TMA located at one of the two three-ring faces.

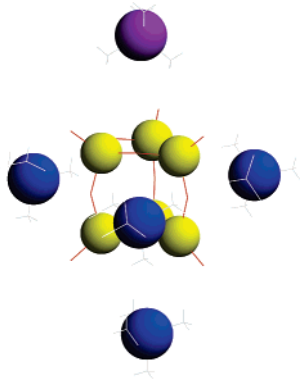

Figure 7. Ball-and-stick image of the prismatic hexamer with five TMA cations: yellow balls, Si atoms; blue balls, N atoms of the restrained TMA cations; magenta ball, N atom of the tagged *TMA* cation that is reversibly pulled off the three-ring face of the surface; red sticks, oxygen atoms; and gray sticks, TMA methyl groups. The image is taken from a molecular dynamics trajectory at the value $R = 6.0$ Å of the reaction coordinate.

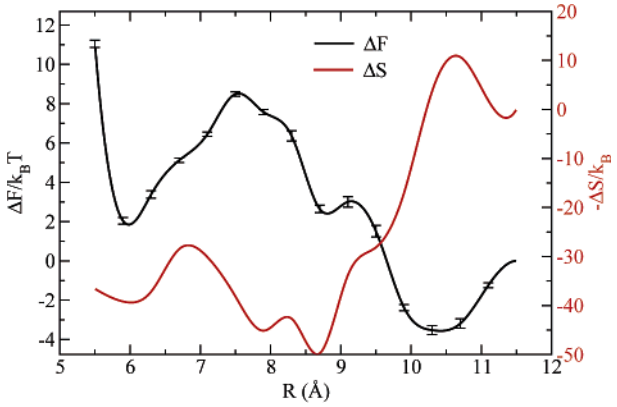

Figure 8. Potential of mean force for the TMA^+ cation−"dressed" prismatic hexamer ion pair, as a function of the ion pair's separation R, in aqueous solution containing five TMA^+ and one Na^+ cations. The black line depicts the potential of mean force, $\Delta F(R)$; the red line depicts the entropic term, $-T\Delta S(R)$, and is drawn on the right-hand scale. (Error bars same as in Figure 1.)

The potential of mean force, $\Delta F(R)$, is given by the black curve in Figure 8. For the hexamer, *TMA* binding is endoergic and the thermodynamically stable state has the *TMA* molecule not bound to the surface of the hexamer but at $R \approx 10.5$ Å from its center. However, the state at $R \approx 6.0$ Å is a local minimum. *TMA* desorption is an activated process over a significant barrier of about $7k_BT$; twice as high as the barrier for single molecule desorption from the surface of the octamer (cf. Figure 3). The relatively high barrier appears consistent with the notion that the hexamer is a rather long-lived metastable species.[16,17,29]

(42) Franks, F.; Reid, D. In *Water, a Comprehensive Treatise*; Franks, F., Ed.; Plenum Press: New York, 1975; Vol. 2, Chapter 5.
(43) Stillinger, F. H. *J. Solution Chem.* **1973**, *2*, 141.

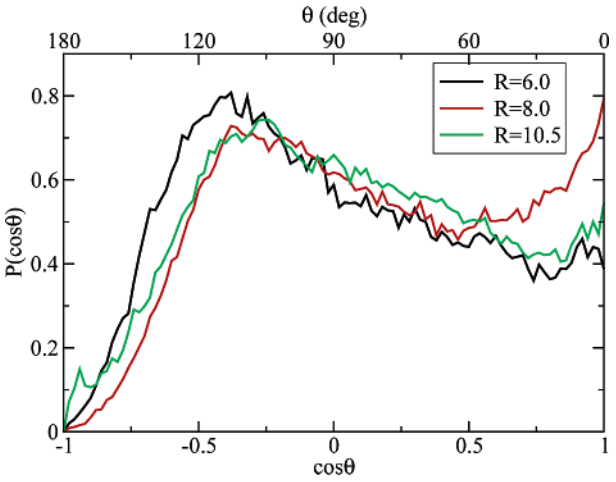

Figure 9. Distribution of orientations of water molecules near the methyl groups of the moving *TMA* cation, at three values of its separation *R* from the center of mass of the hexamer.

Of interest is the entropic contribution, which shows that the endoergic binding is actually entropically *favored*—in stark contrast with our findings for the octamer. The entropy term is depicted by the red curve in Figure 8. Thus, we measure a TMA *desorption* entropy cost of $\Delta S_{des}/k_B \approx -50$ (about -100 cal/(mol K)), from the state at $R \approx 6.0$ to the maximum of $-T\Delta S$ at $R \approx 10.5$ Å.

Analysis of the orientations of *TMA*'s solvation waters gives the distributions shown in Figure 9, in three different states of the system: (i) TMA bound to the surface ($R = 6.0$ Å); (ii) TMA on the desorption barrier ($R = 8.0$ Å); and (iii) TMA in the stable equilibrium state ($R = 10.5$ Å). In the surface-bound state, the distribution $P(\cos\theta)$ (black curve) has a broad peak at $\cos\theta \approx -0.35$. Upon desorption, TMA goes over a significant barrier, where additional solvent joins its solvation sphere. Now, however, the solvation molecules assume configurations with less restrictive geometries. This can be inferred from the two peaks in the corresponding distribution: one at $\cos\theta = 1$, and another, secondary peak at $\cos\theta \approx -0.25$ (cf. red curve). This accounts for the observed entropy increase in the course of *this* transition ($-\Delta S < 0$, in Figure 8). As TMA moves farther from the surface of the hexamer and reaches its equilibrium position ($R = 10.5$), the peak at $\cos\theta = 1$ vanishes again and only the one at $\cos\theta \approx -0.25$ remains (green curve). Thereby, the solvent molecules reorganize into configurations with more restrictive geometries. This accounts for the calculated entropy drop as we move from the barrier to the equilibrium state (cf. Figure 8).

The differences between the two systems, $Q_8^3$and Q_6^3, are obviously not limited to the sign of the free energy of desorption (or binding for that matter) of a TMA-layer molecule. The layer itself behaves quite differently around them. This is evident both from the differences in solvent organization around them and from the concomitant entropy changes that result from TMA binding. We saw that in the case of the octamer there are two reasons for the low entropy of the *TMA*-bound state: first, because true binding necessarily results in ligand translational and rotational freedom losses and, second, because the TMA–octamer complex is of such a size that it allows its solvation molecules to reorganize. By giving up some of their orientational freedom, these waters can keep the integrity of their H-bond network. In fact, the behavior of the "dressed" Q_8^3 in solution is in many respects reminiscent of a hydrophobic solute. In general, solvation of small hydrophobic molecules (surface area ≈ 1 nm^2) entails an entropic cost.[44,45] We have seen, of course, that the water–silicate hydrogen bonds play an integral part in this H-bond network. But we have also seen that these (polar) waters do not sustain any reorganization and thus cannot be responsible for the observed entropic losses [cf. Figure 5, panel b]. The organocations, however, exhibit hydrophobic behavior, and this cannot be ignored. Thus, to some degree, the entropy drop consequent upon TMA binding should be ascribed to the (partly) hydrophobic character acquired by the surface of Q_8^3.

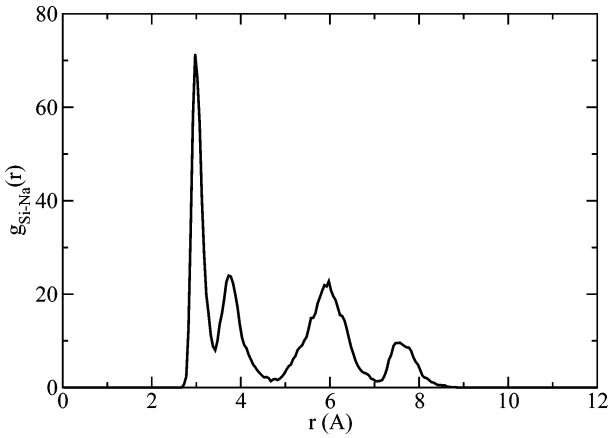

Figure 10. Distribution of Na^+ ions with respect to the cubic octamer.

In other words, the hydrophobic alkyl groups play the important role of organizing the solvent around the cagelike silicates. This type of organization appears to be crucial for the stabilization of the organosilicate complex, not only because such organization facilitates clathrate formation but also because it conduces to the higher-kinetic stability of the H-bonds in the clathrate network.[29]

C. Sodium Ions In Solution. One way to test the last concept and establish the importance of solvent organization in the stabilization of these species, would be to investigate the octamer–TMA ion pair's potential of mean force in the presence of a layer of Na^+ counterions instead of TMA^+. Would TMA^+ still be attracted by the octamer?

To that end, all but one TMA were removed from the simulation box and replaced with seven, randomly placed, Na^+ ions. Under the influence of the strong electric field of the octamer's negative surface charge, the sodium ions quickly settle around it. Unlike TMA, the sodium ions prefer to coordinate more toward the edges rather than directly opposite the faces of the cubic structure. This is clearly reflected in the three major peaks of the pair correlation function $g_{SiNa}(r)$, shown in Figure 10.

It turns out that, under the influence of the layer of sodium counterions, Q_8^3–TMA^+ ion pair binding is *endo*ergic. The calculated pmf is shown in Figure 11. It still has a stationary point at $R = 6.0$ Å, but now it is a local minimum; to reach it, TMA has to climb a substantially high barrier of $\sim 8.0\ k_BT$, at $R \approx 7.5$ Å.

The entropic term $-T\Delta S(R)$ is depicted by the red curve in Figure 11. Like in the case of the hexamer, the exoergic TMA

(44) Chandler, D. *Nature* **2002**, *417*, 491.
(45) Chandler, D. *Nature* **2005**, *437*, 640.

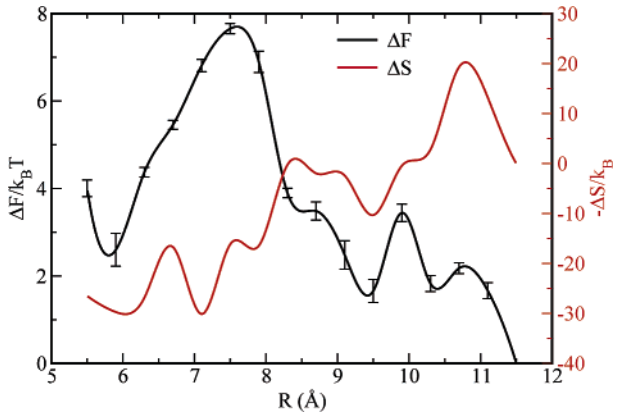

Figure 11. Potential of mean force, $\Delta F(R)$, between a TMA cation and the cubic octamer as a function of the separation R between their centers of mass, in aqueous solution containing seven sodium atoms (black line). The red line depicts the entropic contribution, $-T\Delta S(R)$, and is drawn on the right-hand scale. (Error bars same as in Figure 1.)

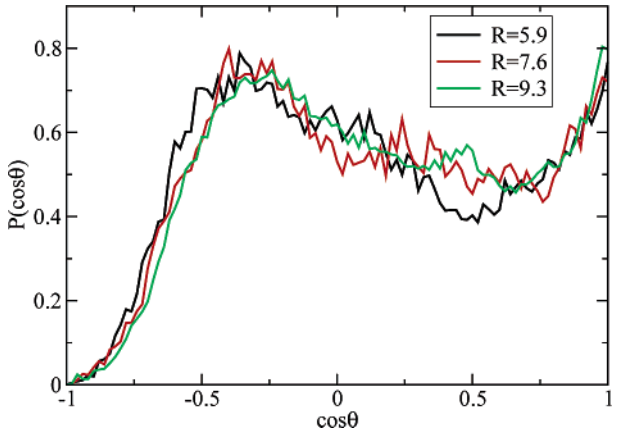

Figure 12. Distribution of orientations of water molecules near the methyl groups of TMA, at various octamer−TMA separations R (in Å)

desorption reaction is followed by an entropy drop $\Delta S_{des}/k_B \approx -30$ (about -60 cal/(mol K)). This entropy change is partly due to the reorganization of the solvation waters of the sodium ions and not those of the TMA and partly due to changes in the H-bond network of the silicate's hydration waters.

Indeed, in Figure 12, we show the distribution, $P(\cos\theta)$, of orientations of TMA's solvation waters, for the three R values 5.9, 7.6, and 9.3 Å, which correspond to the locations of two local minima and of the barrier in between them in $\Delta F(R)$. The three distributions are practically the same, implying minor water reorientation around the organic cation with R.

In Figure 13, we show the water structure around the sodium atoms by plotting the Na−water oxygen pair distribution function, $g_{NaO_w}(r)$. The inner-shell is well-defined and firm, as indicated by the low minimum at $r \approx 3.0$ Å.

In Figure 14, we show the distribution of orientations of those water molecules. (The angle θ is between a water O−H bond and the axis defined by the sodium ion closest to the water molecule and that water's oxygen.) Panel a represents water molecules in the first and second hydration shells; panel b corresponds only to the water molecules in the inner solvation shell. The peak at $\cos\theta \approx 0.5$ corresponds to inner-shell waters; the secondary peak, at $\cos\theta < 0$, corresponds to outer-shell waters and more specifically those around the sodium ions close to TMA^+. As TMA is displaced farther from the surface, the

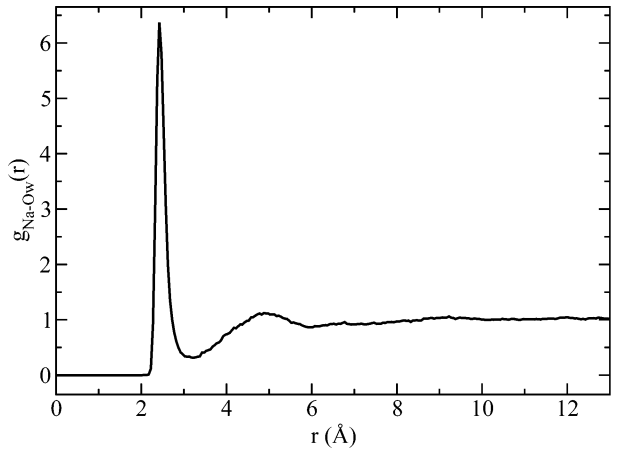

Figure 13. Solvent structure around the sodium cations as inferred from the sodium−water oxygen pair correlation function $g_{NaO_w}(r)$.

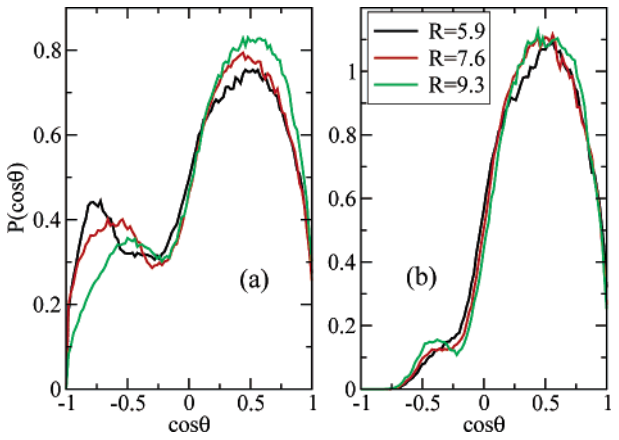

Figure 14. Distribution of orientations of water molecules around the sodium ions, at various octamer−TMA separations R (in Å): (a) distribution includes water molecules in the first and second solvation shells and (b) distribution of orientations of water molecules in the inner solvation shell alone.

solvation waters of those sodium cations progressively reorientate and get aligned with the inner-shell.

It is remarkable how TMA can bind to the surface of the octamer in the presence of a layer of TMA counterions, but cannot do so when this layer is made of sodium cations, despite the fact that in the former system there should be increased steric hindrance, since the TMAs already bound to the surface are much bulkier molecules than the sodium cations. Where could such starkly different behavior be attributed?

The layer of sodium counterions around the octamer disrupt the H-bond network in the neighborhood of the silicate solute. In Figure 15, we show the fractions of water molecules in the vicinity of the octamer that participate in n_{HB} hydrogen bonds, including the water−silicate bonds. Compare this histogram with the one in Figure 4, panel b, which is associated with the octamer with the stable Stern layer of six TMA cations. There is substantial decrease in the fraction of the four-bonded water molecules in favor of the single- and two-bonded ones. The solvent reorganizes but, in this case, not without the breakup of a significant number of water−water hydrogen bonds; this is largely in consequence of solvent polarization induced by the sodium ions. Thereby, the organic cation, which itself induces higher water ordering in its vicinity, cannot be accommodated by the highly polarized environment in the vicinity of

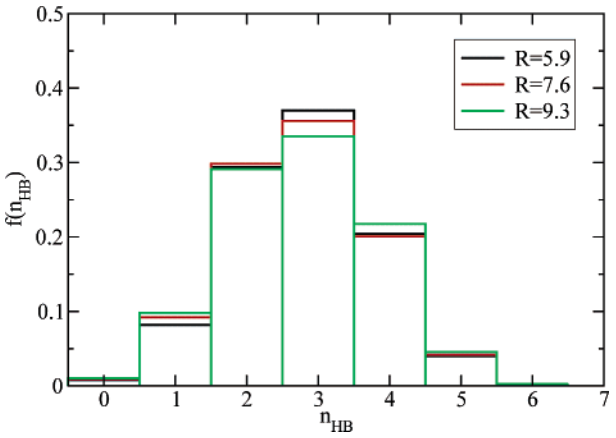

Figure 15. Fraction, $f(n_{HB})$, of water molecules participating in n_{HB} water−water plus water−silicate solute hydrogen bonds at three values of the octamer−TMA separation R (in Å), for the system with one TMA molecule and seven Na^+ ions in solution.

the octamer−sodium complex. The H-bond statistics (and implied solvent organization) depicted by the histogram in Figure 4, panel c are typical of water solvent around a TMA cation.

IV. Discussion

That TAAs play a fundamental role in the growth of symmetrical, cagelike polyions has been shown by kinetic studies and the observed rate law for Q_8^3 growth.[16,17] Unfortunately, the rate law is not enough to unravel the exact mechanism.

A fundamental question we would like an answer to is do TAAs act as templates that organize silicate clathrates around them,[47−50] or do they act as external "scaffolds" that organize the solvent and stabilize the heteronetwork clathrates of oligosilicate-hydrates?[17]

The former requires extensive replacement of water molecules in TAA's solvation sphere by silicate monomers. It has been argued, however, that it is doubtful that water substitution can take place to such an extent as envisaged by the proponents of this idea—it is not supported by the polymerization kinetics.[17] Furthermore, the template theory cannot explain how species like the octamer could form, where the organocation is not inside the cubic structure but outside, forming a layer that is bound to the surface.

On the other hand, the external scaffold theory can rationalize the formation of cagelike species, like the octamer, and, within the same framework, our simulations provide strong support to arguments that try to rationalize their stabilization.

First, it is plausible to assume that silica polymerization and TMA-layer formation do not occur sequentially, with the oligosilicate anions forming first and the TMA layer forming later by adsorption. Rather, it is more likely that organosilicate complexes form by polymerization reactions involving silica monomers which themselves are already part of hydrate clathrates that host the organocations. In this picture, the TAA^+ cations associate with silicate monomers to screen the electrostatic repulsion between the silicate anions (singly or doubly deprotonated $Si(OH)_4$) and thus facilitate or promote the polymerization reaction.[46] It should be noted, however, that the exact nature of this association is still unclear and requires further investigation.

Nevertheless, within the framework of the requisite TAA−silicate association, as condensation proceeds and cagelike species form, the solvation shells of neighboring organocations will inevitably merge, releasing some of the hydrophobically organized water molecules. According to our simulations, stable, cagelike polysilicates require, first, a "continuous" shell of hydrophobic hydration to take on the role of the putative "protective shield" and stave off hydrolysis and, second, *decreased solvent mobility* near the polysilicate anions.

In addition to the hydrophobic hydration shells surrounding the cagelike species, we have shown that there is a very strong hydrogen-bond network between the surrounding waters and the anionic sites of the polysilicate. In the case of the stable species, Q_8^3, we have seen here that these waters, too, exhibit decreased mobility. In fact, as we pointed out earlier, the average lifetime of these hydrogen bonds is intricately related with the presence of a continuous layer of organocations.[29]

Altogether, the organocations play a pivotal role in reorganizing the solvent around the cagelike silicates in a manner conducive to the formation of heteronetwork clathrates that are stable both thermodynamically and kinetically. This solvent reorganization results in entropic losses. Thus, transient species, like the hexamer, that may indeed form but participate in floppy clathrates, eventually have to give way to cagelike polysilicates that lead to more rigid structures, like the octamer.

Within this framework, the stronger evidence in favor of the scaffold theory is provided by our results about the adverse effects of sodium ions on TMA^+ binding. It has been known for a while that using small amounts of alkali-metal cations may accelerate zeolite nucleation and growth.[16,51] The speculation has been that this is probably a consequence of their ability to supplant the organic cations from silicate surfaces. Thereby, the alkali-metal cations weaken the clathrate structure hosting the polysilicate and thus facilitate further polymerization and growth. Our simulations demonstrate for the first time that this is indeed what happens. We have seen here that the sodium counterions quickly settle around the octamer and polarize the local solvent. As a result, they disrupt the local water−water H-bond network, by inducing a substantial decrease in the fraction of the four-bonded water molecules. Eventually, a TMA cation relinquishes its position at the surface of the octamer, because the organic cation, which itself induces higher water ordering in its vicinity, cannot be accommodated by the highly polarized environment.

Can the scaffold theory explain how the TAAs get incorporated in the interior of the zeolite structure?

It has been suggested that, because of electrostatics, some of the solvated TAA^+ cations will ultimately become trapped in the zeolite structure and inevitably serve a space-filling role. While still an open problem, recent work by Lobo and co-workers suggest that this may well be what happens.[20−24] Using in situ SANS and SAXS experiments, the authors have studied the structure of subcolloidal zeolite nanoparticle precursors. They have inferred a core−shell structure, with a TAA^+ shell and a silica core. The resolution in these experiments,

(46) Kinrade, S.; Pole, D. *Inorg. Chem.* **1992**, *31*, 4558.
(47) Chang, C. D.; Bell, A. T. *Catal. Lett.* **1991**, *8*, 305−316.
(48) Burkett, S. L.; Davis, M. E. *J. Phys. Chem.* **1994**, *98*, 4647−4653.
(49) Burkett, S. L.; Davis, M. E. *Chem. Mater.* **1995**, 7, 920−928.
(50) Burkett, S. L.; Davis, M. E. *Chem. Mater.* **1995**, 7, 1453−1463.
(51) Kumar, R.; Bhaumik, A.; Ahedi, R.; Ganapathy, S. *Nature* **1998**, 381, 298.

however, does not allow an unequivocal answer. Molecular simulations should be able to provide very useful information in that respect, but they would have to be carried out on significantly longer scales, both in time and space.

In this and the preceding two papers,[28,29] we have endeavored to elucidate the admittedly multifarious roles of tetraalkylammonium cations in the mechanisms that control the nature and existence of clathrated silicate polyions. It is reasonable to expect that these same mechanisms should also influence zeolite evolution. Altogether, our results do not support the template model but rather the more plausible scaffold model.

As a final thought, we wish to point out that our studies have clearly demonstrated that the stability of the clathrated silicate polyions is intricately connected with solvent dynamics. Modeling of these systems should neither ignore solvent effects nor suppress its molecular structure by treating it merely as a dielectric continuum.

Acknowledgment. Funding for this work was provided by NSF/NIRT (Grant CTS-0103010) and NSF (Grants CTS-0343757, CTS-0522518, and CTS-0327811).

JA064597F